Letter

# Disentangling the influence of excitation energy and compound nucleus angular momentum on fission fragment angular momentum

Simone Cannarozzo,* Stephan Pomp,† Andreas Solders, Ali Al-Adili, Zhihao Gao, and Mattias Lantz
*Department of Physics and Astronomy, Uppsala University, Box 516, 751 20 Uppsala, Sweden*

Heikki Penttilä, Anu Kankainen, Iain Moore, Tommi Eronen, Zhuang Ge, Jouni Ruotsalainen, Maxime Mougeot, Ville Virtanen, Arthur Jaries, Marek Stryjczyk, and Andrea Raggio
*Department of Physics, Accelerator Laboratory, University of Jyvaskyla, P.O. Box 35 (YFL), 40014 Jyvaskyla, Finland*

(Received 6 December 2024; revised 28 January 2025; accepted 7 March 2025; published 26 March 2025)

The origin of the large angular momenta observed for fission fragments is still a question under discussion. To address this, we study isomeric yield ratios (IYRs), i.e., the relative population of two or more long-lived metastable states with different spins, of fission products. We report on IYRs of 17 isotopes produced in the 28-MeV $\alpha$-induced fission of $^{232}$Th at the IGISOL facility of the University of Jyväskylä. The fissioning nuclei in this reaction are $^{233,234,235}$U$^{*}$. We compare our data to IYRs from thermal neutron-induced fission of $^{233}$U and $^{235}$U, and we observe statistically significant larger IYRs in the $^{232}$Th$(\alpha,f)$ reaction, where the average compound nucleus (CN) spin is 7.7 $\hbar$, than in $^{233,235}$U$(n_{\mathrm{th}},f)$, with average spins of 2.6 and 3.6 $\hbar$, respectively. To assess the influence of the excitation energy, we study literature data of IYRs from photon-induced fission reactions, and find that, within current uncertainties, the IYRs indicate no dependency of the CN excitation energy. We conclude that the different IYRs seem to be due to the different CN spins alone. This would imply that the fission fragment angular momentum only partly comes from the fission process itself and is, in addition, influenced by the angular momentum present in the CN.

DOI: 10.1103/PhysRevC.111.L031601

Since its discovery in 1939 [1], considerable progress has been made in advancing our understanding of nuclear fission. However, several fundamental questions remain unresolved [2,3]. One concerns the origin of fission fragment angular momenta, first raised by Wilhelmy *et al.* [4].

In binary fission, after the nucleus reaches the saddle point, two clusters of nucleons begin to form the two nascent fragments. Wilhelmy *et al.* observed that the fragments emerging after scission typically carry significant angular momentum (in the order of 7 $\hbar$ [4]), even in spontaneous fission of the $0^{+}$ spin nucleus $^{252}$Cf. The physical process responsible for the generation of fission fragment (FF) spin is still highly debated [2,5–10].

The two most widely accepted explanations suggest that the angular momentum can be partially determined by the excitation of collective relative orbital motions between the two prefragments before scission [11–14] and/or by Coulomb repulsion around scission [15,16]. At the same time, other factors may also influence the angular momentum generation, such as the deformation of the FFs and the nuclear shell structure [7,17,18].

Recently, Wilson *et al.* proposed postscission generation of the angular momentum [5]. They experimentally observed the same saw-tooth-shaped dependency of the FF angular momentum on the mass for three different low-energy fissioning systems, concluding that completely uncorrelated torques are generated by the rupture of the neck connecting the nascent fragments [5]. However, uncorrelated angular momenta were later also obtained through prescission model calculations by Randrup and Vogt [6] and Scamps and Bertsch [10], showing that the postscission model advanced by Wilson *et al.* [5] is not the only possible explanation for their observation.

Any model describing angular momenta of FFs must account for the influence of both excitation energy and angular momentum of the compound nucleus (CN). The influence of CN conditions on FF spins has been the focus of extensive research, both through experimental activities [5,19–23] and theoretical modeling [8,24,25].

Within the Hauser-Feshbach fission fragment deexcitation model, Kawano *et al.* [24] indeed found indications that FFs from photofission and neutron-induced fission might have similar angular momenta at the same excitation energy of the CN, regardless of its spin. Similarly, in the freya code [8], Vogt and Randrup assume that the main fraction of the CN angular momentum goes into the relative motion of the FFs, while their spin is mainly determined by the temperature of

*Contact author: simone.cannarozzo@physics.uu.se
†Contact author: stephan.pomp@physics.uu.se

*Published by the American Physical Society under the terms of the Creative Commons Attribution 4.0 International license. Further distribution of this work must maintain attribution to the author(s) and the published article's title, journal citation, and DOI. Funded by Bibsam.*

TABLE I. Measured IYR for fission products from $^{232}$Th($\alpha$,$f$) and relevant nuclear data. The values of half-life ($t_{1/2}$), spin ($J$), and excitation energy ($E_{\rm exc}$) were obtained from the Nubase2020 evaluation [35], except for $^{123}$In and $^{123}$Cd, for which more recent values were retrieved from the ENSDF database [36]. Values for half-life and spin are given for ground ($g$) and excited ($e$) state in the isomeric pair. $^{127}$In has two long-lived excited states; however, in this work, only the ground state and the 394-keV, $J = 1/2^-$ state are considered.

| Nucleus | $t_{1/2,g}$ (s) | $J_g$ ($\hbar$)] | $E_{\rm exc}$ (keV) | $t_{1/2,e}$ (s) | $J_e$ ($\hbar$) | IYR |
|---|---|---|---|---|---|---|
| $^{97}$Y | 3.75(3) | 1/2− | 667.5(2) | 1.17(3) | 9/2+ | 0.800(5) |
| $^{99}$Nb | 15.0(2) | 9/2+ | 365.27(8) | 150(10) | 1/2− | 0.732(8) |
| $^{119}$Cd | 161(1) | 1/2+ | 146.5(1) | 132(1) | 11/2− | 0.836(5) |
| $^{121}$Cd | 13.5(3) | 3/2+ | 214.9(1) | 8.3(8) | 11/2− | 0.834(5) |
| $^{123}$Cd | 2.1(3) | 3/2+ | 144(4) | 1.8(3) | 11/2− | 0.85(1) |
| $^{125}$Cd | 0.68(4) | 3/2+ | 186(4) | 0.48(3) | 11/2− | 0.86(1) |
| $^{119}$In | 144(6) | 9/2+ | 311.37(3) | $1.08(2) \times 10^3$ | 1/2− | 0.948(3) |
| $^{121}$In | 23.1(6) | 9/2+ | 313.68(7) | 233(6) | 1/2− | 0.947(5) |
| $^{123}$In | 6.17(5) | 9/2+ | 327.21(4) | 47.4(8) | 1/2− | 0.958(3) |
| $^{125}$In | 2.36(4) | 9/2+ | 352(12) | 12.2(2) | 1/2− | 0.933(3) |
| $^{127}$In | 1.086(7) | 9/2+ | 394(12) | 3.62(2) | 1/2− | 0.873(3) |
| $^{129}$Sn | 134(2) | 3/2+ | 35.15(5) | 414(6) | 11/2− | 0.80(1) |
| $^{132}$Sb | 167(4) | 4+ | 150(50) | 246(3) | 8− | 0.41(1) |
| $^{133}$Te | 750(20) | 3/2+ | 334.26(4) | $3.32(2) \times 10^3$ | 11/2− | 0.708(7) |
| $^{132}$I | $8.26(5) \times 10^3$ | 4+ | 110(11) | $4.99(5) \times 10^3$ | 8− | 0.59(2) |
| $^{134}$I | $3.15(1) \times 10^3$ | 4+ | 316.5(2) | 211(2) | 8− | 0.715(7) |
| $^{136}$I | 83.4(4) | 1− | 206(15) | 47(1) | 6− | 0.692(8) |

the fissioning nucleus at scission. Furthermore, within the framework of a fully microscopical model, Bulgac *et al.* showed [25] that an increase in the compound nucleus excitation energy might produce FFs at higher spins. They concluded that the average spin of the FFs increases with the kinetic energy of the incident neutrons in the fission reactions of $^{235}$U and $^{239}$Pu.

From an experimental perspective, Bulgac *et al.*'s result is supported by Refs. [19,21,22], which report an increase of the $\gamma$-ray multiplicity as a function of the kinetic energy of the incident neutrons in the fission reactions of $^{238}$U and $^{239}$Pu.

A different way of looking for correlations is to use the spin-trap isomers of the produced nuclei. The fission products (FPs), after the neutron evaporation and the $\gamma$-ray cascade, eventually decay into a (meta)stable nuclear state, before further $\beta$ decay towards the line of stability. A large number of nuclei have more than one long-lived metastable state, differing in spin and excitation energy. The angular momentum of a FF influences the population of the isomeric states [26,27]. Therefore, the ratio between the production rate of two or more long-lived metastable states, the so-called isomeric yield ratio (IYR), provides access to the angular momentum of fission fragments [4,28–34].

In this work, we investigate how the CN state affects the angular momentum of FFs by making use of the IYR and the assumption of a positive correlation between the FFs' spin and the population of high-spin isomeric states in the observed fission products.

We define the IYR as

$$\mathrm{IYR} = \frac{Y_{\rm hs}}{Y_{\rm hs} + Y_{\rm ls}}, \tag{1}$$

where $Y_{\rm hs}$ and $Y_{\rm ls}$ are the fission product yields of the high-spin and low-spin states for an isomeric pair.

We study comparable fissioning nuclei using both new IYR data from our measurement of the 28-MeV $\alpha$-induced fission of $^{232}$Th (see Table I and Fig. 1) and literature data retrieved from the EXFOR experimental nuclear data library [37]. Using 28-MeV $\alpha$ particles, the CN formed by $^{232}$Th($\alpha$,$f$), i.e., $^{236}$U$^*$, may emit one or two prescission neutrons. The probabilities of the first-, second-, and third-chance fission calculated using the nuclear model codes talys v2.0 [38] and gef v3.3 [39], are listed in Table II, together with the corresponding average excitation energies. One can also produce $^{236}$U$^*$ and $^{234}$U$^*$ via thermal neutrons impinging on $^{235}$U and $^{233}$U, respectively. In both cases the excitation energy is approximately 6 MeV.

According to optical model calculations with talys using default parameters, the CN produced by a 28-MeV $\alpha$ particle impinging on $^{232}$Th has an average angular momentum of 7.7 $\hbar$, as shown in Fig. 2. We assume that prescission neutrons do not, on average, change the spin of the system, an assumption commonly made in studies of deexciting fission fragments. The thermal ($s$-wave) neutrons produce $^{236}$U$^*$ and $^{234}$U$^*$ with average angular momenta of about 3.6 and 2.6 $\hbar$ (Fig. 2), respectively. Therefore, the CNs produced in these three fission

TABLE II. Probability of first- to third-chance fission for the 28-MeV $\alpha$-induced fission of $^{232}$Th, as calculated by talys ($P_T$) and gef ($P_G$), and corresponding average excitation energies ($\overline{E}_T$, $\overline{E}_G$).

| Scissioning Nucleus | $P_T$(%) | $P_G$(%) | $\overline{E}_T$(MeV) | $\overline{E}_G$(MeV) |
|---|---|---|---|---|
| $^{236}$U$^*$ | 24 | 21 | 23.0 | 23.0 |
| $^{235}$U$^*$ | 35 | 41 | 14.9 | 15.4 |
| $^{234}$U$^*$ | 40 | 37 | 8.4 | 8.9 |

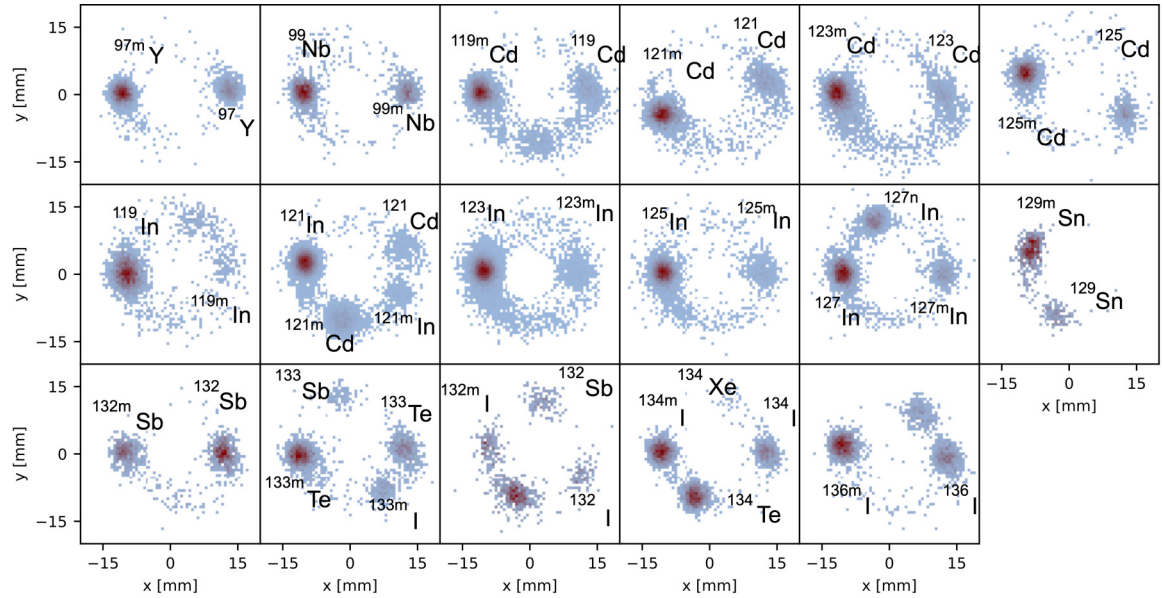



FIG. 1. PI-ICR images produced during the experimental campaign. Identified nuclei are marked in the plots. A number of pictures show the presence of contaminants and asymmetrical tails (see Fig. 3). Phase-accumulation times were optimized to ensure that the regions of interest do not overlap with other ion species.

reactions are similar but carry significantly different angular momenta. We assume that these distributions represent the angular momenta of those nuclei that actually undergo fission.

While IYR from thermal neutron-induced fission reactions have been measured for several nuclei, the corresponding data for $\alpha$-induced fission of $^{232}$Th is scarce [40] with only one measurement for $^{131}$Te and $^{133}$Te [41]. The IYR for $^{133}$Te reported in Ref. [41] differs significantly from our result. This is likely due to limitations in their measurement method, which requires significant corrections based on fission yields and decay data.

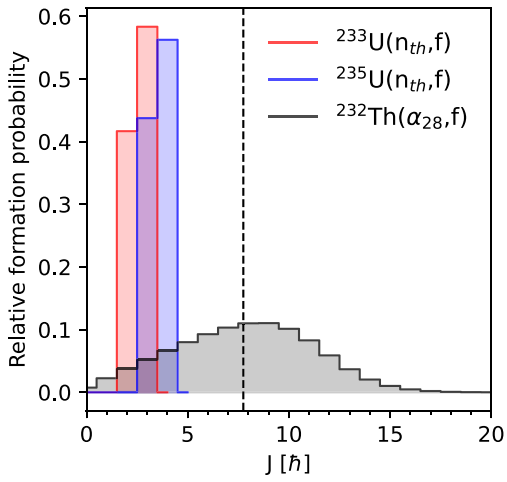



FIG. 2. Relative formation probabilities of CN angular momenta resulting from the three considered reactions. The average values are 2.6 and 3.6 $\hbar$ for $^{234}$U$^*$ and $^{236}$U$^*$, respectively, when produced from thermal neutrons, and 7.7 $\hbar$ for $^{236}$U$^*$ produced from incident $\alpha$ particles at 28 MeV.

We measured 17 IYRs from the $^{232}$Th($\alpha$,$f$) reaction using the phase-imaging ion-cyclotron-resonance (PI-ICR) technique of the JYFLTRAP double Penning trap mass spectrometer, at the IGISOL-4 facility [33,42,43]. The technique has previously been used to measure IYRs [32,44,45], is applicable for isomeric states with half-lives longer than approximately 500 ms, and can resolve states separated by 30–40 keV, or more. The obtained data are presented in Table I. Out of these, 16 have been measured for this system for the first time.

In the experiment, 32-MeV $\alpha$ particles from the K-130 cyclotron were directed to a $^{232}$Th target with a thickness of 10 mg/cm$^2$. The average $\alpha$-particle kinetic energy in the thorium target was estimated to be 28 MeV. In the stopping cell of the fission ion guide (see, e.g., Ref. [46]), primary ions from the fission reactions were stopped and extracted by a purified helium gas flow at 300 mbar. Due to the high-ionization potential of helium, the FPs are not neutralized in this process, allowing them to be accelerated to 30 keV using an electrostatic potential.

The formed ion beam was mass separated using a 55° dipole magnet with a mass resolution $M/\Delta M$ of approximately 500. The continuous beam was collected in a cooler and buncher [47], where it was bunched for high-precision mass analysis in the JYFLTRAP double Penning trap [48]. In a first step, as much of the contaminants as possible was removed from the ion bunch in the first trap using the mass-selective buffer-gas cooling method [49]. In the second trap, the PI-ICR technique [50] was applied. First the ion motion was excited with a short (1 ms) dipolar oscillating electric field at the ions' reduced cyclotron frequency in order to initiate the mass-dependent revolution of the ions in the trap. Over time, ions with different masses separate due to their different eigenfrequencies. After a preset waiting time, a quadrupole

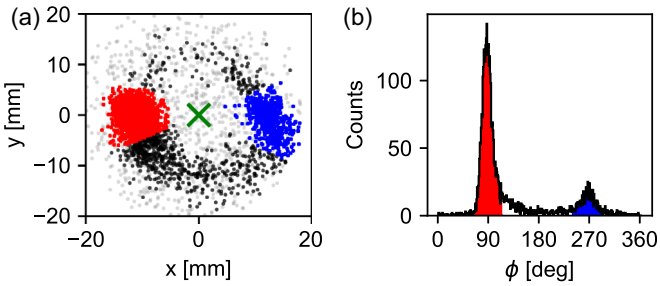



FIG. 3. (a) PI-ICR image for $^{123}$Cd, and (b) polar projection of the detected ions. In blue and red, respectively, the ions identified as high- and low-spin isomeric states are shown.

excitation at the ions free-space cyclotron frequency $\nu_c = \frac{1}{2\pi}\frac{q}{m}B$ is used to convert the fast mass-dependent cyclotron motion to the slow magnetron motion. This "freezes" the relative position of the ions, which are extracted and detected in a position-sensitive detector, as illustrated in Figs. 1 and 3.

The two spots are formed by the detected nuclei of interest in the two isomeric states. The method to assign the spots to the corresponding isomeric state is explained in detail in Refs. [31,44]. For both spots, the ions detected within $3\sigma$ from the center of the peaks in the polar projection [Fig. 3(b)] are used to calculate the number of counts in the spot. In some cases, the spots in PI-ICR images show asymmetric tails. The physics origin of these is still unclear, but is likely due to ion-ion interactions. In this measurement, the number of ions in these tails is on the order of 1–5% of the number of ions in the corresponding spot. To account for the presence of the tails, different methods to count the detected ions were tested, and in cases where the methods resulted in different values, the uncertainty was increased to enfold all data.

Each measurement was performed a second time, where the position of the spots on a micro-channel plate detector (MCP) was interchanged to minimize the corrections for inhomogeneities in the MCP detection efficiency. Following the definition of IYR given in Eq. (1), we calculate the ratio between the number of observed ions in either state extracted from the trap as $\mathrm{IYR_{exp}} = C_{\mathrm{hs}}/(C_{\mathrm{hs}} + C_{\mathrm{ls}})$, where $\mathrm{IYR_{exp}} = C_{\mathrm{hs}}/(C_{\mathrm{hs}} + C_{\mathrm{ls}})$ and $C_{\mathrm{ls}}$ are the number of counts associated with the high-spin and low-spin isomeric states, respectively. The two $\mathrm{IYR_{exp}}$ were eventually merged into an average value.

If the half-lives of the nuclei of interest or their $\beta$-decay precursors are similar to the measurement cycle (0.5–1 s), a relevant fraction of them will have time to decay before detection. The procedure to correct for this started with an assumed value for the isomeric ratio after fission, i.e., the true IYR. The ion transport was simulated by discretizing the transport time into time steps, and evaluating, for each, a balance equation for the isomeric states of the ion of interest and its precursors. This process was iterated, adjusting the trial ratio until the resulting calculated IYR matched the experimental one. Bootstrapping is used to determine the IYR and its uncertainty. Details are presented in Ref. [51].

The measured IYRs from the present study are listed in Table I and shown in Fig. 4. Except for $^{132}$Sb, all nuclei show a dominant feeding of the high-spin state, i.e., an IYR

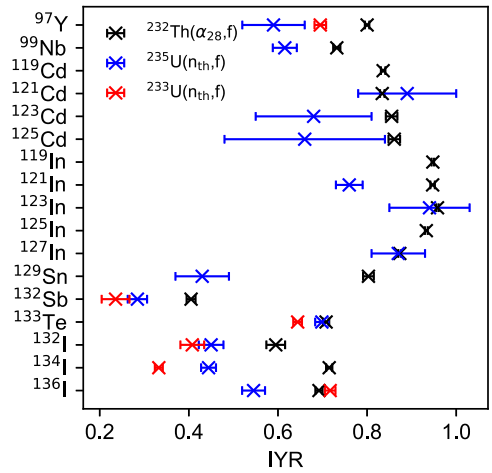



FIG. 4. Weighted average value of experimental IYRs in literature for thermal neutron-induced fission of $^{233}$U (red) and $^{235}$U (blue) compared to the $^{232}$Th data.

larger than 0.5. Figure 4 also shows the comparison between the IYRs measured in this study and those measured in the neutron-induced fission reactions retrieved from literature data, where the EXFOR data are averaged into one data point for each nucleus and fissioning system. The $^{232}$Th IYR data consistently show values larger than those of the $^{233}$U and $^{235}$U data (Fig. 4). The weighted means of the difference between experimental and literature data are $\Delta\mathrm{IYR} = 0.135(8)$ and 0.156(6) for $^{235}$U and $^{233}$U, respectively. Normalizing with the change in CN spin as described above (from 7.7 $\hbar$ to 3.6 and 2.6 $\hbar$), we arrive at $\Delta\mathrm{IYR}/\Delta\bar{J} = 0.032(1)\ \hbar^{-1}$ for the studied isomeric pairs. The Wilcoxon signed-rank test suggests a significant difference between our measurements and the literature values ($p = 9 \times 10^{-4}$) for $^{235}$U, and a strong trend towards a difference ($p = 6.25 \times 10^{-2}$) for $^{233}$U. These data show that the higher-spin CNs produced by $^{232}$Th($\alpha$,$f$) tend to promote more frequent deexcitation to higher-spin isomeric states.

The used literature data have been obtained with techniques different from the one employed in our work, typically using $\gamma$-ray spectroscopy. If provided, we use reported independent IYRs but chose to include also cumulative IYRs in Fig. 4 and the derived numerical values. We verified that a restriction to independent IYRs gives, within the uncertainties, the same results. Direct ion counting is a more advanced technique for measuring IYRs (see, e.g., Ref. [32]), and the difference in measurement methodology may explain some of the observed differences. However, the found difference in $\Delta$IYR for the two thermal-fission cases as given above is 0.02(1), while directly comparing the two cases gives 0.03(1). Since the difference in the average CN spin is 1 $\hbar$, these values are in line with the proposed trend. Nevertheless, the reported values can only serve as preliminary estimates of a IYR dependency on the angular momentum of the compound nucleus.

To isolate and study the influence of the excitation energy of the CN on the angular momentum of FFs, we compare literature data for the IYRs of several FPs produced in

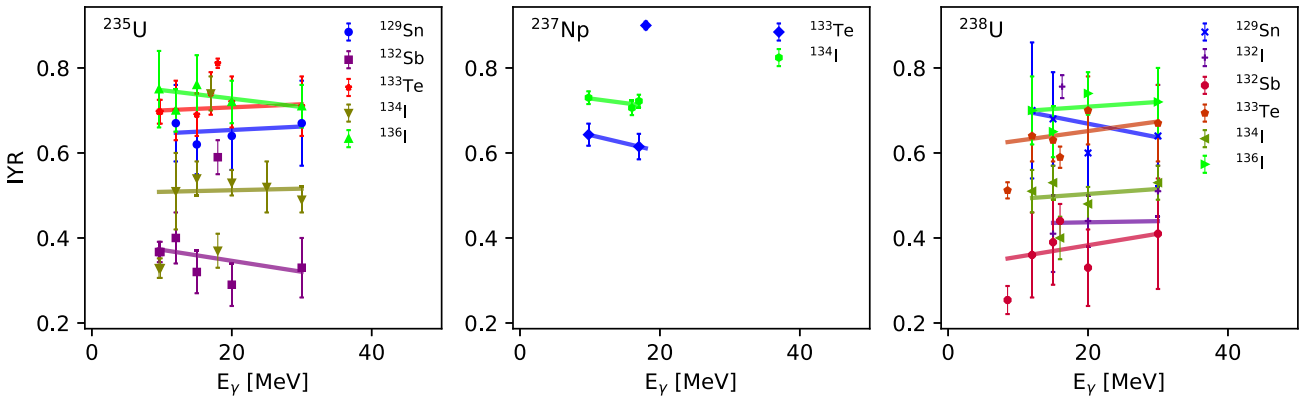



FIG. 5. Isomeric yield ratios from photofission for the isotopes in this study. The IYRs are extracted from EXFOR [37] and plotted as a function of incident photon energy for different fissioning systems. Solid lines represent the linear regressions of the experimental data, where the Huber loss function [52] is used in order to have a regression robust to outliers. Only reactions with more than three energy data-points are included.

photon-induced fission reactions as a function of the energy of the incident photons. In fission reactions induced by photons in the few tens of MeV range, the excitation energy of the CN increases as a function of the incident photon energy while its spin remains mainly unchanged.

Figure 5 shows IYRs for the nuclei in this study for photon-induced fission reactions, as a function of the incident photon energy for different fissioning systems. These bibliographic data are retrieved from EXFOR [37]. We obtain an average slope of $\Delta\mathrm{IYR}/\Delta E = 0.0001(5)\ \mathrm{MeV}^{-1}$; i.e., we see no effect of the incident photon energy on the IYR. This implies that the angular momenta of the FFs seem to remain unaffected by an increase in the CN excitation energy.

Part of the additional excitation energy can be carried away by neutrons before and after scission. Therefore, this observation also implies that neutron emission does not, at least not on average, remove a significant amount of angular momentum. This agrees with the result by Gjestvang *et al.* [20] and the common assumption that statistical neutrons carry away a negligible amount of angular momentum. This has, however, recently been questioned by Stetcu *et al.* [53] for postscission neutrons.

To summarize, we provide experimental evidence that an increase of the spin of the compound system undergoing fission leads to an increase in the population of the high-spin state of an isomeric pair. Based on the literature [26,27], we conclude that this is due to an increase in the FF angular momentum. While this might, at least in part, also be due to a change in excitation energy of the fissioning nucleus, our study of IYRs from photofission suggests that this is not the case. In fact, the photofission data provide no evidence of any influence of the excitation energy on the IYR and, therefore, the FF angular momentum.

If confirmed, this would contradict the results from the modeling of the momentum generation in freya [8], but would agree with the theoretical and experimental observations of Refs. [19,21–23,25]. PI-ICR measurements of IYRs from thermal-neutron-induced fission of $^{233,235}$U would be highly desirable and could clarify the situation.

In their research, Wilson *et al.* [5] studied neutron-induced fission of $^{232}$Th and $^{238}$U at about 2-MeV incident energy, as well as spontaneous fission of $^{252}$Cf. From their results they concluded that a FF's angular momentum does not depend on the fissioning system. The same lack of dependency is observed by Sears *et al.* [40] in their IYR compilation. They show, for a number of thermal neutron-induced fission reactions, that the measured IYRs do not depend on the mass of the fissioning nuclei. However, the considered reactions dominantly have small CN angular momenta. Combining these findings with our results would imply that, while a part of the FF angular momentum comes from the fission process itself, it is also influenced by the angular momentum present in the CN.

Based on our results, one can estimate a lower limit of the additional angular momentum of a FF that is due to an increase in CN angular momentum. Using the talys code, we have estimated the additional angular momentum that a FF needs to have to increase the observed IYR by 0.15. We found that, on average, this increase needs to be at least one unit of $\hbar$. This would imply that at least 2 $\hbar$ out of the additional 4–5 $\hbar$ (i.e., $>40\%$) goes to the FFs' angular momenta, while a maximum of 3 $\hbar$(i.e., $<60\%$) is converted into orbital angular momentum or dissipated via emission of prefission neutrons. A detailed calculation could be done using methods outlined in Refs. [31,33,34]. The values given here should be considered as a conservative estimate of a lower limit.

Finally, we note that the data may suggest a possible dependency of the observed IYR increase on the FP mass, which may be less pronounced in the region of symmetric fission. This could mean that a larger portion of the additional angular momentum is transmitted to the FFs in asymmetric fission compared to symmetric fission. To investigate this hypothesis, more data are needed for isotopes in the region around mass number $A = 116$, where several suitable isomers exist.

We acknowledge the staff of the Accelerator Laboratory of University of Jyväskylä (JYFL-ACCLAB) for providing a stable online beam. We express gratitude for the fruitful

discussions with Toshihiko Kawano. This work was supported by the Swedish Research Council (Ref. No. 2020-04238) and has received funding from the Euratom Research and Training Program 2014-2018 under Grant No. 847594 (ARIEL). We acknowledge support from the Research Council of Finland under Grants No. 295207, No. 327629, and No. 354968 and the European Union's Horizon 2020 Research and Innovation Programme under Grants No. 771036 (ERC CoG MAIDEN) and No. 861198-LISA-H2020-MSCA-ITN-2019.

The data that support the findings of this article which are not available in the paper itself are available from the authors upon reasonable request.

[1] O. Hahn and F. Strassmann, Naturwissenschaften **27**, 11 (1939).
[2] A. N. Andreyev, K. Nishio, and K.-H. Schmidt, Rep. Prog. Phys. **81**, 016301 (2018).
[3] K.-H. Schmidt and B. Jurado, Rep. Prog. Phys. **81**, 106301 (2018).
[4] J. B. Wilhelmy, E. Cheifetz, R. C. Jared, S. G. Thompson, H. R. Bowman, and J. O. Rasmussen, Phys. Rev. C **5**, 2041 (1972).
[5] J. N. Wilson, D. Thisse, M. Lebois, N. Jovančević, D. Gjestvang, R. Canavan, M. Rudigier, D. Étasse, R.-B. Gerst, L. Gaudefroy, E. Adamska, P. Adsley, A. Algora, M. Babo, K. Belvedere, J. Benito, G. Benzoni, A. Blazhev, A. Boso, S. Bottoni *et al.*, Nature (London) **590**, 566 (2021).
[6] J. Randrup and R. Vogt, Phys. Rev. Lett. **127**, 062502 (2021).
[7] P. Marević, N. Schunck, J. Randrup, and R. Vogt, Phys. Rev. C **104**, L021601 (2021).
[8] R. Vogt and J. Randrup, Phys. Rev. C **103**, 014610 (2021).
[9] A. Bulgac, Phys. Rev. C **106**, 014624 (2022).
[10] G. Scamps and G. Bertsch, Phys. Rev. C **108**, 034616 (2023).
[11] J. Rasmussen, W. Nörenberg, and H. Mang, Nucl. Phys. A **136**, 465 (1969).
[12] L. G. Moretto, G. F. Peaslee, and G. J. Wozniak, Nucl. Phys. A **502**, 453 (1989).
[13] A. Bulgac, I. Abdurrahman, K. Godbey, and I. Stetcu, Phys. Rev. Lett. **128**, 022501 (2022).
[14] T. Døssing, S. Åberg, M. Albertsson, B. G. Carlsson, and J. Randrup, Phys. Rev. C **109**, 034615 (2024).
[15] M. M. Hoffman, Phys. Rev. **133**, B714 (1964).
[16] J. Randrup, Phys. Rev. C **108**, 064606 (2023).
[17] B. D. Wilkins, E. P. Steinberg, and R. R. Chasman, Phys. Rev. C **14**, 1832 (1976).
[18] G. F. Bertsch, T. Kawano, and L. M. Robledo, Phys. Rev. C **99**, 034603 (2019).
[19] N. P. Giha, S. Marin, J. A. Baker, I. E. Hernandez, K. J. Kelly, M. Devlin, J. M. O'Donnell, R. Vogt, J. Randrup, P. Talou, I. Stetcu, A. E. Lovell, O. Litaize, O. Serot, A. Chebboubi, C.-Y. Wu, S. D. Clarke, and S. A. Pozzi, Phys. Rev. C **107**, 014612 (2023).
[20] D. Gjestvang, J. N. Wilson, A. Al-Adili, S. Siem, Z. Gao, J. Randrup, D. Thisse, M. Lebois, N. Jovančević, R. Canavan, M. Rudigier, D. Étasse, R.-B. Gerst, E. Adamska, P. Adsley, A. Algora, C. Belvedere, J. Benito, G. Benzoni, A. Blazhev *et al.*, Phys. Rev. C **108**, 064602 (2023).
[21] L. Qi, M. Lebois, J. N. Wilson, A. Chatillon, S. Courtin, G. Fruet, G. Georgiev, D. G. Jenkins, B. Laurent, L. Le Meur, A. Maj, P. Marini, I. Matea, L. Morris, V. Nanal, P. Napiorkowski, A. Oberstedt, S. Oberstedt, C. Schmitt, O. Serot *et al.*, Phys. Rev. C **98**, 014612 (2018).
[22] J.-M. Laborie, R. Billnert, G. Bélier, A. Oberstedt, S. Oberstedt, and J. Taieb, Phys. Rev. C **98**, 054604 (2018).
[23] D. C. Aumann, W. Gückel, E. Nirschl, and H. Zeising, Phys. Rev. C **16**, 254 (1977).
[24] T. Kawano, A. E. Lovell, S. Okumura, H. Sasaki, I. Stetcu, and P. Talou, Phys. Rev. C **107**, 044608 (2023).
[25] A. Bulgac, I. Abdurrahman, S. Jin, K. Godbey, N. Schunck, and I. Stetcu, Phys. Rev. Lett. **126**, 142502 (2021).
[26] R. Vandenbosch and J. R. Huizenga, Phys. Rev. **120**, 1313 (1960).
[27] J. R. Huizenga and R. Vandenbosch, Phys. Rev. **120**, 1305 (1960).
[28] H. Naik, T. Datta, S. P. Dange, P. K. Pujari, S. Prakash, and M. V. Ramaniah, Z. Phys. A: At. Nucl. **331**, 335 (1988).
[29] H. Naik, S. Dange, R. Singh, and T. Datta, Nucl. Phys. A **587**, 273 (1995).
[30] H. Naik, R. Singh, S. Dange, and W. Jang, Appl. Radiat. Isot. **208**, 111304 (2024).
[31] V. Rakopoulos, M. Lantz, A. Solders, A. Al-Adili, A. Mattera, L. Canete, T. Eronen, D. Gorelov, A. Jokinen, A. Kankainen, V. S. Kolhinen, I. D. Moore, D. A. Nesterenko, H. Penttilä, I. Pohjalainen, S. Rinta-Antila, V. Simutkin, M. Vilén, A. Voss, and S. Pomp, Phys. Rev. C **98**, 024612 (2018).
[32] V. Rakopoulos, M. Lantz, S. Pomp, A. Solders, A. Al-Adili, L. Canete, T. Eronen, A. Jokinen, A. Kankainen, A. Mattera, I. D. Moore, D. A. Nesterenko, M. Reponen, S. Rinta-Antila, A. de Roubin, M. Vilén, M. Österlund, and H. Penttilä, Phys. Rev. C **99**, 014617 (2019).
[33] A. Al-Adili, V. Rakopoulos, and A. Solders, Eur. Phys. J. A **55**, 61 (2019).
[34] Z. Gao, A. Solders, A. Al-Adili, S. Cannarozzo, M. Lantz, S. Pomp, and H. Sjöstrand, Phys. Rev. C **109**, 064626 (2024).
[35] F. Kondev, M. Wang, W. Huang, S. Naimi, and G. Audi, Chin. Phys. C **45**, 030001 (2021).
[36] National Nuclear Data Center, from ENSDF database as of Feb. 2, 2024, version available at http://www.nndc.bnl.gov/ensarchivals/, accessed: 2/21/24.
[37] N. Otuka, E. Dupont, V. Semkova, B. Pritychenko, A. Blokhin, M. Aikawa, S. Babykina, M. Bossant, G. Chen, S. Dunaeva, R. Forrest, T. Fukahori, N. Furutachi, S. Ganesan, Z. Ge, O. Gritzay, M. Herman, S. Hlavač, K. Katō, B. Lalremruata *et al.*, Nucl. Data Sheets **120**, 272 (2014).
[38] A. Koning, A. Hilaire, and S. Goriely, Eur. Phys. J. A **59**, 131 (2023).
[39] K.-H. Schmidt, B. Jurado, C. Amouroux, and C. Schmitt, Nucl. Data Sheets **131**, 107 (2016).
[40] C. Sears, A. Mattera, E. McCutchan, A. Sonzogni, D. Brown, and D. Potemkin, Nucl. Data Sheets **173**, 118 (2021).
[41] T. Datta, S. M. Sahakundu, S. P. Dange, N. Chakravarty, R. Guin, and S. Prakash, Phys. Rev. C **28**, 1206 (1983).
[42] S. Eliseev, K. Blaum, M. Block, C. Droese, M. Goncharov, E. Minaya Ramirez, D. A. Nesterenko, Y. N. Novikov,

and L. Schweikhard, Phys. Rev. Lett. **110**, 082501 (2013).

[43] I. Moore, T. Eronen, D. Gorelov, J. Hakala, A. Jokinen, A. Kankainen, V. Kolhinen, J. Koponen, H. Penttilä, I. Pohjalainen, M. Reponen, J. Rissanen, A. Saastamoinen, S. Rinta-Antila, V. Sonnenschein, and J. Äystö, Nucl. Instrum. Methods Phys. Res. Sect. B **317**, 208 (2013).

[44] Z. Gao, A. Solders, A. Al-Adili, O. Beliuskina, T. Eronen, A. Kankainen, M. Lantz, I. Moore, D. Nesterenko, H. Penttilä, S. Pomp, and H. Sjöstrand, Eur. Phys. J. A **59**, 169 (2023).

[45] Z. Gao, A. Solders, A. Al-Adili, S. Cannarozzo, M. Lantz, S. Pomp, O. Beliuskina, T. Eronen, S. Geldhof, A. Kankainen, I. D. Moore, D. Nesterenko, and H. Penttilä (IGISOL Collaboration), Phys. Rev. C **108**, 054613 (2023).

[46] H. Penttilä, V.-V. Elomaa, T. Eronen, J. Hakala, A. Jokinen, A. Kankainen, I. Moore, S. Rahaman, S. Rinta-Antila, J. Rissanen, V. Rubchenya, A. Saastamoinen, C. Weber, and J. Äystö, Eur. Phys. J. A **48**, 43 (2012).

[47] A. Nieminen, J. Huikari, A. Jokinen, J. Äystö, P. Campbell, and E. Cochrane, Nucl. Instrum. Methods Phys. Res. Sect. A **469**, 244 (2001).

[48] T. Eronen, V. S. Kolhinen, V.-V. Elomaa, D. Gorelov, U. Hager, J. Hakala, A. Jokinen, A. Kankainen, P. Karvonen, S. Kopecky, I. D. Moore, H. Penttilä, S. Rahaman, S. Rinta-Antila, J. Rissanen, A. Saastamoinen, J. Szerypo, C. Weber, and J. Äystö, Eur. Phys. J. A **48**, 46 (2012).

[49] G. Savard, S. Becker, G. Bollen, H.-J. Kluge, R. Moore, T. Otto, L. Schweikhard, H. Stolzenberg, and U. Wiess, Phys. Lett. A **158**, 247 (1991).

[50] D. A. Nesterenko, T. Eronen, Z. Ge, A. Kankainen, and M. Vilen, Eur. Phys. J. A **57**, 302 (2021).

[51] S. Cannarozzo, Isomeric yield ratio studies in nuclear reactions and alpha-particle induced fission of thorium, Licentiate thesis, Uppsala University, Uppsala, 2023.

[52] P. J. Huber, Ann. Math. Stat. **35**, 73 (1964).

[53] I. Stetcu, A. E. Lovell, P. Talou, T. Kawano, S. Marin, S. A. Pozzi, and A. Bulgac, Phys. Rev. Lett. **127**, 222502 (2021).